Original Article

Association between oncogenic RAS mutation and radiologic-pathologic findings in patients with primary rectal cancer

Sung Jae Jo, Seung Ho Kim

Department of Radiology, Inje University College of Medicine, Haeundae Paik Hospital, Haeundae-gu, Busan, Korea

Correspondence to: Seung Ho Kim, MD. Department of Radiology, Inje University College of Medicine, Haeundae Paik Hospital, Haeundae-ro 875, Haeundae-gu, Busan 612-030, Korea. Email: radiresi@gmail.com.

Background: To evaluate the association between various radiologic-pathologic findings and oncogenic Kirsten-ras (KRAS) mutation in patients with primary rectal cancer.

Methods: Seventy-five patients with primary rectal cancer who had undergone rectal magnetic resonance imaging (MRI) were included. The rectal MRI consisted of T2-weighted images in three planes, pre- and post-contrast-enhanced T1-weighted images, and axial diffusion-weighted images (b factors, 0, 1,000 s/mm^2). Two radiologists reviewed the MRI scans and measured the axial and longitudinal tumor lengths (LTLs), apparent diffusion coefficient (ADC), and relative contrast enhancement [signal intensity (SI) difference of tumor on pre- and post-contrast T1WI/SI of tumor on pre-contrast T1WI]. The associations among the qualitative data (tumor stage, node stage, lymphatic invasion, venous invasion, and perineural invasion), quantitative data (tumor length, ADC, relative contrast enhancement) and KRAS mutations were statistically analyzed by Fisher's exact test for the qualitative data and by the Mann-Whitney U test for the quantitative data. An area under receiver operating characteristic curve (AUC) was considered as the diagnostic performance for the prediction of KRAS mutation. Molecular-biologic results served as the reference standard.

Results: The ratio of axial to LTL in the KRAS-mutant group (n=41) was higher than that in the wild-type group (n=34) (0.29±0.15; 0.22±0.08, P=0.0117). The AUC was 0.640 (95% CI, 0.520 to 0.747, P=0.0292) with an estimated maximum accuracy of 64%. The mean ADC of the mutant group was not significantly different from that of the wild-type group [(0.95±0.17)×10^{-3} mm^2/s; (0.96±0.17)×10^{-3} mm^2/s, P=0.6505]. The relative contrast enhancement showed no significant difference between the two groups (1.66±0.93, 1.35±0.84, P=0.1581). The other qualitative findings also did not show any significant difference (P>0.05).

Conclusions: The ratio of axial to LTL showed a significant difference according to KRAS mutation in patients with primary rectal cancer. However, it showed a low accuracy of 64% for prediction of KRAS mutation.

Keywords: Magnetic resonance imaging (MRI); apparent diffusion coefficient (ADC); Kirsten-ras (KRAS) mutation; rectal neoplasms; relative contrast enhancement

Submitted Oct 13, 2018. Accepted for publication Dec 19, 2018.
doi: 10.21037/qims.2018.12.10
View this article at: http://dx.doi.org/10.21037/qims.2018.12.10

Introduction

Colorectal cancer (CRC) is associated with a variety of environmental, genetic and epigenetic factors and arises due to a combination of these factors (1). CRC has well-known genetic mechanisms (2,3) that are exploited clinically for individualized patient treatments. There have been many studies on targeted treatments and the factors that can predict response to them (4-8). Representative among these treatments are anti-epidermal growth factor receptor (EGFR) antibody therapy and oncogenic Kirsten-ras

(KRAS) mutation (5-8). Anti-EGFR monoclonal antibodies are therapeutic agents that can prolong survival in patients who have not responded to conventional treatments (9). KRAS is an oncogene that forms an EGFR signaling cascade through various pathways including Ras-Raf-MARK (10). Through these pathways, KRAS modifies cell transformation and inhibits the tumor suppressor pathways. When KRAS mutations, which are found in 30–40% of CRC patients, are present, these pathways are activated continuously, which makes anti-EGFR monoclonal antibodies less effective in blocking EGFR (5-7,11). Studies have shown that patients with KRAS-mutant tumors did not benefit from anti-EGFR antibody therapy (5,6). Therefore, the presence of KRAS mutation in CRC is of great importance for determination of individualized treatment.

Although pretreatment magnetic resonance imaging (MRI) has been widely performed for local tumor staging and treatment planning in rectal cancer, few studies have investigated the association between KRAS mutations and MRI-based radiologic findings (12,13). Furthermore, because the qualitative radiologic parameters were subjective and the accuracy of MRI for nodal staging in particular was quite variable, these results are limited from a clinical implementation standpoint (14,15). Therefore, the aim of our study was to investigate the associations among quantitative radiologic parameters [i.e., tumor length, relative contrast enhancement and apparent diffusion coefficient (ADC)], qualitative histopathologic results (i.e., tumor stage, node stage, venous invasion, lymphatic invasion, perineural invasion), and molecular-biologic KRAS mutations in patients with primary rectal cancer.

Methods

This retrospective study was approved by the relevant institutional review board, and informed consent was waived.

Patients and selection criteria

Between June 2010 and October 2017, 759 patients were surgically and histopathologically confirmed as rectal adenocarcinoma. The data from 98 of these patients who satisfied the inclusion criteria were collected. The inclusion criteria were as follows: (I) patients who underwent preoperative rectal MRI and (II) patients who had documentation of KRAS mutation. Twenty-three patients who had undergone neoadjuvant chemo-radiation therapy prior to surgery were excluded. Finally, 75 patients (male: 48, female: 27, mean age: 69 years, range, 37–87 years) were enrolled in the study.

MRI

All of the MRI examinations were performed with a 3.0-T magnetic resonance machine (Achieva, Philips Medical Imaging, Best, Netherlands) with a phased-array body coil (Torso-pelvis coil, USA Instruments, Aurora, OH, USA). For optimal distension of the rectum, the rectum was filled with approximately 50–80 mL of ultrasound gel (Ecosonic, Sanipia, Korea) just prior to the examination. To minimize bowel motility, one vial (20 mg) of scopolamine butylbromide (Buscopan, Boehringer Ingelheim, Germany) was injected intravenously 10 minutes prior to the scan, if not contraindicated.

The MRI protocol consisted of axial, coronal and sagittal T2-weighted turbo spin-echo sequences (T2WI), axial pre- and post-contrast T1-weighted sequences (T1WI) with spectral pre-saturation by inversion recovery, and diffusion-weighted imaging (DWI) sequences by the single-shot echo planar imaging technique. The sagittal T2WI was obtained first in order to identify the longest tumor axis, followed by the axial and coronal images perpendicular and parallel to the tumor axis. DWI (b values of 0 and 1,000 s/mm^2) was taken parallel to the axial T2WI. Gadoterate meglumine (Dotarem, Guerbet, Aulnay-Sous-Bois, France) was used as the contrast agent. The contrast-agent dose was the routine 0.2 mL/kg administered by automated contrast injector (Spectris MR, Medrad Europe, Maastricht, The Netherlands) at a rate of 3 mL/s. A total of 25 mL of saline flushing was performed at the same rate. Post-contrast T1WI was obtained 60 seconds after contrast-agent injection. The detailed sequence parameters for each sequence are summarized in *Table 1*.

Image analysis

All of the MRI scans were reviewed on a picture archiving and communication system (PACS) workstation (m-view, Marotech, Seoul, Korea). Two radiologists, with 15 and 3 years' experience of assessing rectal MRI, reviewed the MRI scans. Blinded to the presence of KRAS mutation and the relevant histopathologic results, they determined each tumor's location, border, and 3 dimensions by consensus. After determining the dimensions and border, the radiologist with 3 years' experience measured the maximum axial and longitudinal tumor lengths (LTLs) on the axial

Table 1 MRI sequence parameters

Parameters	T2-weighted axial, sagittal, and coronal TSE	Pre- and post-contrast-enhanced axial T1-weighted imaging	DWI (b =0, 1,000 s/mm^2)
TR (ms)	3,727	500–600	9,500
TE (ms)	90	11	65
ETL	17	5	73
Slice thickness (mm)	3	3	2
Slice gap (mm)	0.3	0.3	0
Matrix size	300×290	300×300	120×118
NEX	1	2	10
FOV (mm)	240×240	240×240	240×240
Acquisition time	2 min 30 s	3 min 20 s–3 min 59 s	5 min 40 s
No. of slices	40	40	70

T1-weighted imaging was performed using the spectral pre-saturation with inversion recovery (SPIR) technique; diffusion-weighted imaging (DWI) was performed using the single-shot echo planar imaging technique. TR, repetition time; TE, echo time; ETL, echo train length; FOV, field of view; NEX, number of excitations; TSE, turbo spin echo.

and sagittal planes, respectively. The maximum axial tumor length (ATL) was defined as the distance from the inner edge to the outer edge of the tumor including extramural tumor growth. The maximum LTL was defined as the distance between the upper margin and lower margin of the tumor. The radiologist also measured, for each tumor, the ADC value and relative contrast enhancement. For the ADC measurement, the radiologist identified each tumor on axial T2WI and DWI and manually drew regions of interest (ROIs) along the tumor border on DWI cross-sectional slices. The mean ADC value of each tumor was obtained by the copying and pasting of the aforementioned ROIs to a corresponding ADC map and averaging. Similarly, for relative contrast enhancement of the tumor, the manually drawn ROIs were also located in order to cover and measure the whole tumor's signal intensity (SI) on pre- and post-contrast-enhanced T1WI. The relative contrast enhancement was calculated by the following equation: (post-contrast SI – pre-contrast SI)/pre-contrast SI.

Histopathologic analysis

All of the specimens were obtained by surgical resection. They were assessed by one dedicated pathologist for the following histopathologic findings: (I) KRAS mutation; (II) T stage; (III) N stage; (IV) tumor invasion (lymphatic, venous and perineural invasion). The T stage and N stage were determined according to the staging classification of the seventh edition of the American Joint Committee on Cancer (16).

Evaluation for KRAS mutation

KRAS mutations in CRC occur most frequently in codons 12 and 13, which account for 95% of all mutation types, and less frequently in codons 61, 146 and 154 (17).

Genomic DNA was extracted from tumor-tissue-containing paraffin sections using the QIA amp DNA Mini kit (Qiagen, Hilden, Germany). Polymerase chain reaction and pyrosequencing were performed to evaluate the KRAS mutations in codons 12, 13 (exon 2) and 61 (exon 3). The sequence data were generated with the ABI PRISM 3730 DNA analyzer (Applied Biosystems, Foster City, CA, USA) and analyzed by Sequencing analysis software version 5.1.1 (Applied Biosystems, Foster City, CA, USA) for comparison of the variations.

Statistical analysis

The ADC and relative contrast-enhancement data from the mucinous tumors were excluded from the analysis, because mucinous tumors show remarkably high ADC values and poor enhancement compared with non-mucinous tumors (18). The Mann-Whitney U test was used to

Table 2 Histopathologic stages of study population

Stages	T1	T2	T3	T4	Total
N0	5	16	19	2	42
N1	0	5	12	0	17
N2	0	0	14	2	16
Total	5	21	45	4	75

assess the associations between the quantitative radiologic parameters and the presence of KRAS mutation. Associations between the categorical data among the histopathologic findings and the presence of KRAS mutation were assessed using Fisher's exact test. A receiver operating characteristic curve (ROC) analysis was performed to evaluate the discriminatory power of the ratio of axial to longitudinal tumor length (ATL/LTL) for the prediction of KRAS mutation by calculating the area under the ROC curve (AUC). An optimal cut-off value for maximum accuracy was calculated with an estimated sensitivity, specificity, positive predictive value (PPV) and negative predictive value (NPV). The threshold for statistical significance among the results was a P value <0.05. The statistical analyses were carried out using MedCalc software for Windows (MedCalc software version 12.7.1.0, Mariakerke, Belgium).

Results

Demographics of study population

Among the 75 patients, KRAS mutation was detected in 41 patients (55%; hereafter, the mutant group) and not detected in 34 patients (45%; hereafter, the wild-type group). The mutations were found on codons 12 (n=31), 13 (n=11), and 61 (n=1). Two patients showed simultaneous KRAS mutations (codons 12 and 13, and codons 13 and 61, respectively). Mucinous adenocarcinoma was histopathologically revealed in nine patients, among whom, seven patients had the KRAS mutation and two patients did not. The final pathologic stages of the study population are summarized in *Table 2*.

Quantitative analysis

The ATL/LTL was significantly higher in the KRAS-mutant group than in the wild-type group (0.29±0.15; 0.22±0.08, P=0.0117) (*Figures 1* and *2*). The AUC of the ATL/LTL was 0.640 (95% CI, 0.520 to 0.747, P=0.0292) (*Figure 3*). The optimal cut-off value was 0.26 with a maximum accuracy of 64%, sensitivity of 51%, specificity of 79%, PPV of 75% and NPV of 57%. However, there was no significant difference between the two groups in terms of the other length parameters (e.g., ATL and LTL; P=0.0758 and P=0.4161, respectively). With respect to the ADC value, no significant difference was found between the two groups [mutant: $(0.95\pm0.17)\times10^{-3}$ mm^2/s; wild type: $(0.96\pm0.17)\times10^{-3}$ mm^2/s, P=0.6505]. Regarding the relative contrast enhancement, there was no significant difference between the two groups (mutant: 1.66±0.93; wild type: 1.35±0.84, P=0.1581). The detailed data on the association between the quantitative radiologic data and KRAS mutation are summarized in *Table 3*.

Qualitative analysis

No significant differences were found between the two groups with respect to lymphatic invasion (P=0.6060), venous invasion (P=0.7871), or perineural invasion (P=1). Tumor stage and lymph node stage also did not show any significant difference between the two groups (P=0.4536). The associations between the histopathological data and KRAS mutation are summarized in *Table 4*.

Discussion

In this study, the ATL/LTL in the KRAS-mutant group was significantly higher than that in the wild-type group. This result is in concordance with Shin's study, which revealed an association between radiologic findings and KRAS mutation in primary rectal cancer (12). The authors also observed that the ATL/LTL showed a significant difference between the two groups (mutant: 0.46±0.29; wild type: 0.36±0.20; P=0.0090) (12). Our result also corresponds well with the results of previous studies showing significantly higher frequencies of KRAS mutation in CRC having a polypoid or upward growth pattern (19-22). These findings suggest that KRAS mutation is associated with morphologic tumor growth patterns. Increased cell growth activity induced by activated KRAS mutation seems to be essential for polypoid growth in CRC (21,23,24). These observations support the present findings that the axial, and not longitudinal, dimension of tumors tended to be larger in the KRAS-mutant group than in the wild-type group. However, the ATL/LTL showed a limited accuracy for the prediction of KRAS mutation. Recently, MR-based radiomics has

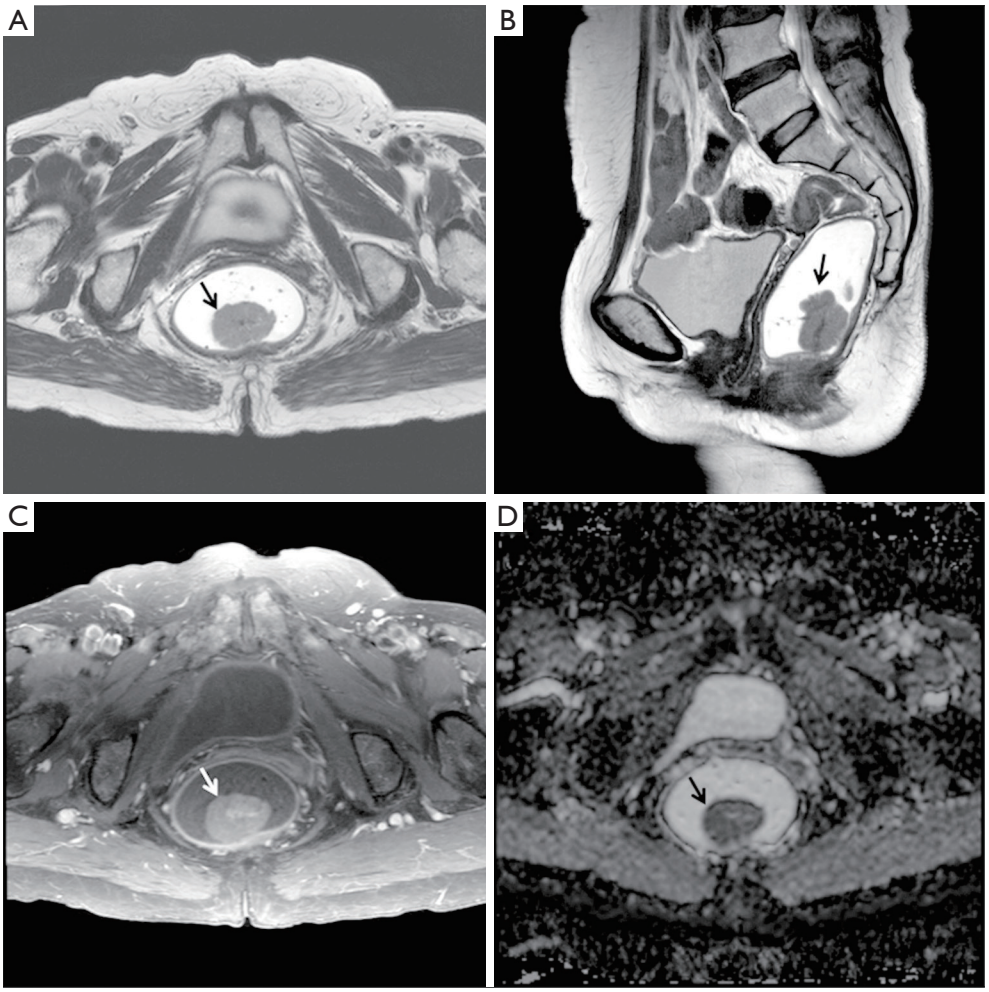

Figure 1 MRI scans of a 70-year-old woman diagnosed with rectal adenocarcinoma (T1N0M0) with KRAS mutation. (A) T2-weighted axial and (B) sagittal images show a polypoid mass (arrow) arising from the lower rectum. The ratio of axial to longitudinal tumor length was 0.80 (2.8 cm/3.5 cm). (C) An axial contrast-enhanced fat-suppressed T1-weighted image also shows the polypoid mass (arrow) with mild enhancement. The relative contrast-enhancement ratio was 0.46. (D) On an ADC map (b factor, 1,000 s/mm^2), the ADC value of the tumor (arrow) was 0.972×10^{-3} mm^2/s. ADC, apparent diffusion coefficient.

been investigated to improve diagnostic, prognostic and predictive accuracy for rectal cancer (25,26). Further studies are warranted to aid in identifying a potential imaging biomarker among quantitative radiologic parameters on KRAS mutation in rectal cancer.

The mean ADC values in this study did not show a significant difference between the two groups [mutant: (0.95±0.17)×10^{-3} mm^2/s; wild type: (0.96±0.17)×10^{-3} mm^2/s; P=0.6505], which accords with a previous result based on a large study population (n=275) (12). The authors also demonstrated that the ADC values were not different between the two groups [mutant: (0.96±0.23)×10^{-3} mm^2/s; wild type: (0.97±0.21)×10^{-3} mm^2/s; P=0.6230] (12). By contrast, other investigators have reported significantly lower mean ADC values in a KRAS-mutant group relative to a wild-type group [mutant: (1.26±0.36)×10^{-3} mm^2/s; wild type: (1.43±0.22)×10^{-3} mm^2/s; P=0.01] (13). However, due to the small study population of the KRAS-mutant group (n=13), the authors of that report cautioned against drawing any firm conclusions on their ADC value discrepancy. We believe that further such studies on ADC values according to KRAS-mutation status are necessary before any solid

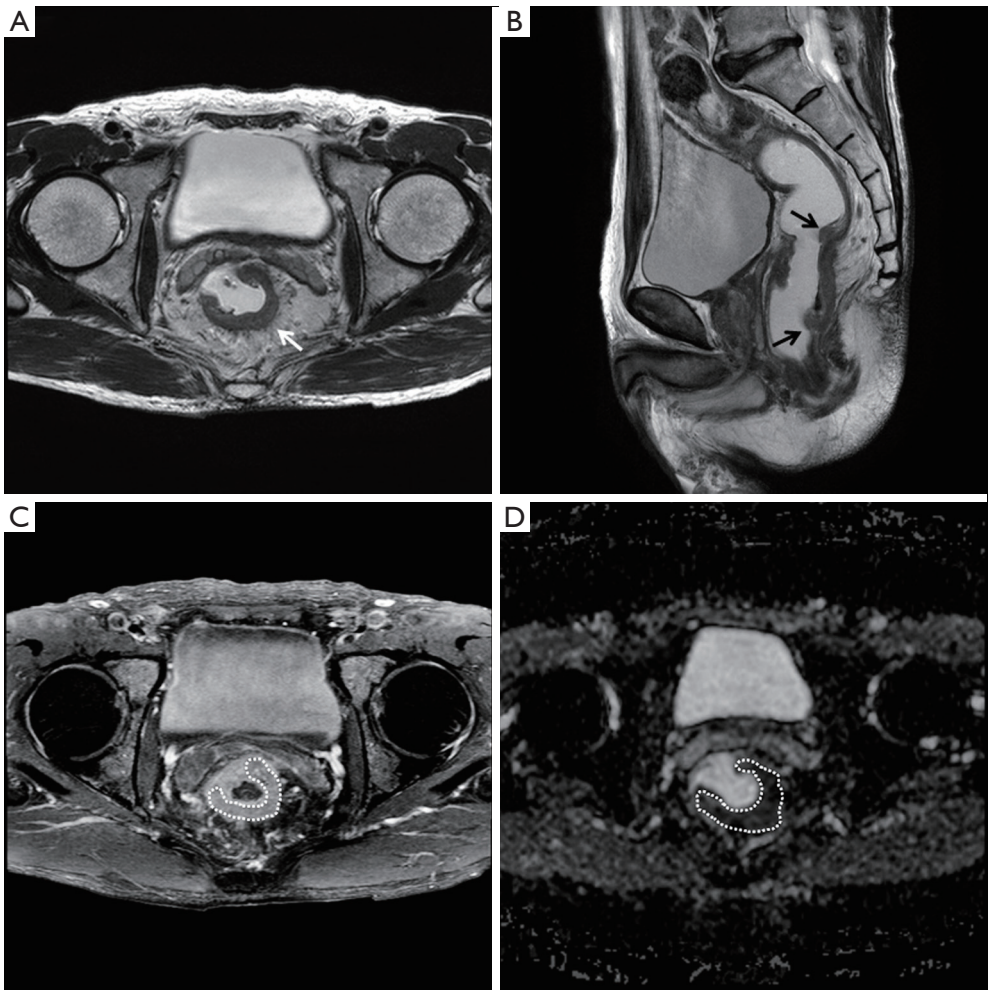

Figure 2 MRI scans of a 62-year-old man diagnosed with rectal adenocarcinoma (T3N1bM0) without KRAS mutation. (A) T2-weighted axial and (B) sagittal images show an ulcero-infiltrative mass (arrows) in the mid rectum. The ratio of axial to longitudinal tumor length was 0.20 (1.5 cm/7.5 cm). (C) An axial contrast-enhanced fat-suppressed T1-weighted image also shows the ulcero-infiltrative mass (dotted line) with moderate enhancement. The relative contrast enhancement ratio was 1.48. (D) On an ADC map (b factor, 1,000 s/mm^2), the ADC value of the tumor (dotted line) was 0.974×10^{-3} mm^2/s. ADC, apparent diffusion coefficient.

consensus can be reached.

Regarding our relative contrast enhancement, it did not show a significant difference between the two groups (mutant: 1.66±0.93; wild type: 1.35±0.84; P=0.1581). Shin *et al.*'s qualitative evaluation of tumor enhancement according to KRAS-mutation status likewise found no significant intergroup difference (P=0.3545) (12). However, in contrast to our study, the authors used an arbitrary classification. Specifically, homogeneous or heterogeneous enhancement was categorized by a cutoff value of 50% of tumor volume. Beyond the scope of relative contrast enhancement, a quantitative dynamic contrast-enhanced MRI study using perfusion parameters demonstrated a tendency toward a higher K^{trans} (a volume transfer constant also known as a major perfusion parameter) in a KRAS-mutant group than in a wild-type group (0.123±0.032; 0.100±0.039, respectively; P=0.060) (27). Previous studies have investigated the correlation of perfusion parameters with biologic features such as tumor angiogenesis (27-29). It is known that tumor angiogenesis arises from upregulation of vascular endothelial growth factor, which is possibly associated with KRAS mutation (30). Therefore, KRAS-mutation status can be used to assess tumor angiogenesis.

With regard to our other radiologic findings, tumor,

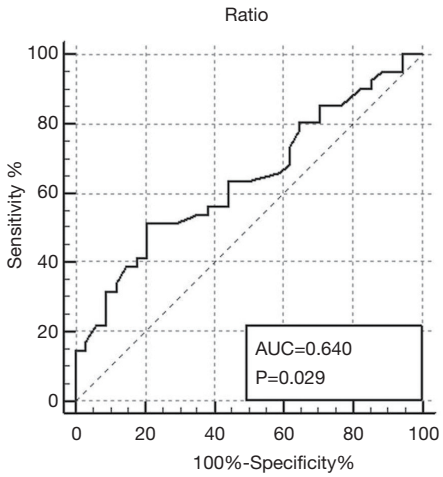

Figure 3 Receiver operating characteristic curve of the ratio of axial to longitudinal tumor length for predicting KRAS mutation. KRAS, Kirsten-ras.

node stage and extramural venous invasion (EMVI) did not show any significant difference between the two groups. Shin *et al.* observed a significantly higher node stage in their KRAS-mutant group than in their wild-type group (P=0.0064); however, they found no significant differences in terms of tumor stage or EMVI (P=0.4731 and 0.4364, respectively) (12). Such controversial results might be due to the wide range of accuracy and poor inter-observer agreement for node stage in subjective visual assessment of MRI scans. Therefore, in the present study, objective histopathologic tumor and node stage, along with EMVI, were applied to the analyses to verify the previous results that were based on radiologic interpretation alone (12).

There are several limitations to this study. First, the study design was retrospective, and the study population was relatively small. Because of the small sample size of the mucinous tumor population (7 mutants and 2 wild types),

Table 3 Association between quantitative radiologic data and KRAS mutation

Parameters	KRAS mutation (N=41)	KRAS wild type (N=34)	P
ATL (cm)	1.36±0.85	1.09±0.38	0.0758
LTL (cm)	5.03±2.07	5.42±2.06	0.4161
ATL/LTL	0.29±0.15	0.22±0.08	0.0117
ADC† ($\times 10^{-3}$ mm^2/s)	0.95±0.17	0.96±0.17	0.6505
Relative contrast enhancement†	1.66±0.93	1.35±0.84	0.1581

Data are mean ± standard deviation (SD). †, ADC values and relative contrast enhancement were measured and analyzed only in non-mucinous tumors. ATL, axial tumor length; LTL, longitudinal tumor length; ADC, apparent diffusion coefficient; KRAS, Kirsten-ras.

Table 4 Association between histopathologic data and KRAS mutation

Parameters	KRAS mutation (N=41) (%)	KRAS wild type (N=34) (%)	P
Lymphatic invasion			
Yes	10/21 (47.6)	11/21 (52.4)	0.6060
No	31/54 (57.4)	23/54 (42.6)	
Venous invasion			
Yes	9/18 (50.0)	9/18 (50.0)	0.7871
No	32/57 (56.1)	25/57 (43.9)	
Perineural invasion			
Yes	17/32 (53.1)	15/32 (46.9)	1
No	24/43 (55.8)	19/43 (44.2)	

KRAS, Kirsten-ras.

statistical analysis was not possible. Thus, any definite findings concerning the mucinous subtype could not be included in the final assessment. Therefore, inherent selection bias might have resulted. However, in an effort to avoid this possibility, we enrolled patients consecutively. Second, we measured the static SI in the portal venous phase rather than the dynamic perfusion parameters that are potential biomarkers for evaluation of tumor contrast enhancement; as such, we could not find any association between perfusion parameters and KRAS mutation. Third, we evaluated only KRAS-mutation status. It is well known that CRC results from a combination of genetic and epigenetic factors (1). Other genetic and epigenetic biomarkers, such as BRAF (v-raf murine sarcoma viral oncogene homolog B1), APC (adenomatous polyposis coli), loss of SMAD (small mothers against decapentaplegic) activity and LOH (loss of heterozygosity) of 17p and 18q, are known to be associated with advanced-stage and poor prognosis of rectal cancer (1). Although KRAS has been thought to be associated with advanced-stage cancer, a recent study found that patients with specific KRAS mutation of isolated p.G12A had aggressive disease (stage III or IV, with extensive metastatic or recurrent disease) (31). Thus, other gene statuses or specific KRAS mutations might have influenced our results, and those should be further investigated.

In conclusion, the ATL/LTL showed a significant difference according to KRAS mutation in patients with primary rectal cancer. However, it showed a low accuracy of 64% for prediction of KRAS mutation.

Acknowledgements

Funding: This work was supported by the GUERBET Korea Research grant (GK-DTR-2018-36).

Footnote

Conflicts of Interest: The authors have no conflicts of interest to declare.

Ethical Statement: This retrospective study was approved by the relevant institutional review board, and informed consent was waived.

References

1. Coppedè F, Lopomo A, Spisni R, Migliore L. Genetic and epigenetic biomarkers for diagnosis, prognosis and treatment of colorectal cancer. World J Gastroenterol 2014;20:943-56.
2. Arnold CN, Goel A, Blum HE, Boland CR. Molecular pathogenesis of colorectal cancer: implications for molecular diagnosis. Cancer 2005;104:2035-47.
3. Rajagopalan H, Nowak MA, Vogelstein B, Lengauer C. The significance of unstable chromosomes in colorectal cancer. Nat Rev Cancer 2003;3:695-701.
4. Russo AL, Borger DR, Szymonifka J, Ryan DP, Wo JY, Blaszkowsky LS, Kwak EL, Allen JN, Wadlow RC, Zhu AX, Murphy JE, Faris JE, Dias-Santagata D, Haigis KM, Ellisen LW, Iafrate AJ, Hong TS. Mutational analysis and clinical correlation of metastatic colorectal cancer. Cancer 2014;120:1482-90.
5. Karapetis CS, Khambata-Ford S, Jonker DJ, O'Callaghan CJ, Tu D, Tebbutt NC, Simes RJ, Chalchal H, Shapiro JD, Robitaille S, Price TJ, Shepherd L, Au HJ, Langer C, Moore MJ, Zalcberg JR. K-ras mutations and benefit from cetuximab in advanced colorectal cancer. N Engl J Med 2008;359:1757-65.
6. Sorich MJ, Wiese MD, Rowland A, Kichenadasse G, McKinnon RA, Karapetis CS. Extended RAS mutations and anti-EGFR monoclonal antibody survival benefit in metastatic colorectal cancer: a meta-analysis of randomized, controlled trials. Ann Oncol 2015;26:13-21.
7. Lièvre A, Bachet JB, Boige V, Cayre A, Le Corre D, Buc E, Ychou M, Bouchè O, Landi B, Louvet C, Andrè T, Bibeau F, Diebold MD, Rougier P, Ducreux M, Tomasic G, Emile JF, Penault-Llorca F, Laurent-Puig P. KRAS mutations as an independent prognostic factor in patients with advanced colorectal cancer treated with cetuximab. J Clin Oncol 2008;26:374-79.
8. Qiu LX, Mao C, Zhang J, Zhu XD, Liao RY, Xue K, Li J, Chen Q. Predictive and prognostic value of KRAS mutations in metastatic colorectal cancer patients treated with cetuximab: a meta-analysis of 22 studies. Eur J Cancer 2010;46;2781-7.
9. Jonker DJ, O'Callaghan CJ, Karapetis CS, Zalcberg JR, Tu D, Au HJ, Berry SR, Krahn M, Price T, Simes RJ, Tebbutt NC, van Hazel G, Wierzbicki R, Langer C, Moore MJ. Cetuximab for the treatment of colorectal cancer. N Engl J Med 2007;357:2040-8.
10. Baselga J. The EGFR as a target for anticancer therapy—focus on cetuximab. Eur J Cancer 2001;37:S16-22.
11. Lovinfosse P, Koopmansch B, Lambert F, Jodogne S, Kustermans G, Hatt M, Visvikis D, Seidel L, Polus M, Albert A, Delvenne P, Hustinx R. (18)F-FDG PET/

CT imaging in rectal cancer: relationship with the RAS mutational status. Br J Radiol 2016;89:20160212.
12. Shin YR, Kim KA, Im S, Hwang SS, Kim K. Prediction of KRAS mutation in rectal cancer using MRI. Anticancer Res 2016;36:4799-804.
13. Xu Y, Xu Q, Sun H, Liu T, Shi K, Wang W. Could IVIM and ADC help in predicting the KRAS status in patients with rectal cancer? Eur Radiol 2018;28:3059-65.
14. Bipat S, Glas AS, Slors FJ, Zwinderman AH, Bossuyt PM, Stoker J. Rectal cancer: local staging and assessment of lymph node involvement with endoluminal US, CT, and MR imaging—a meta-analysis. Radiology 2004;232:773-83.
15. Lahaye MJ, Engelen SM, Nelemans PJ, Beets GL, van de Velde CJ, van Engelshoven JM, Beets-Tan RG. Imaging for predicting the risk factors—the circumferential resection margin and nodal disease—of local recurrence in rectal cancer: a meta-analysis. Semin Ultrasound CT MR 2005;26:259-68.
16. Edge SB, Byrd DR, Compton CC, Fritz AG, Greene FL, Trotti A. editors. AJCC cancer staging manual. 7th ed. New York: Springer-Verlag, 2010.
17. Tan C, Du X. KRAS mutation testing in metastatic colorectal cancer. World J Gastroenterol 2012;18:5171-80.
18. Nasu K, Kuroki Y, Minami M. Diffusion-weighted imaging findings of mucinous carcinoma arising in the ano-rectal region: comparison of apparent diffusion coefficient with that of tubular adenocarcinoma. Jpn J Radiol 2012;30:120-7.
19. Chiang JM, Chou YH, Chou TB. K-ras codon 12 mutation determines the polypoid growth of colorectal cancer. Cancer Res 1998;58:3289-93.
20. Kaneko K, Fujii T, Kato S, Boku N, Oda Y, Koba I, Ohtsu A, Hosokawa K, Ono M, Shimoda T, Yoshida S. Growth patterns and genetic changes of colorectal carcinoma. Jpn J Clin Oncol 1998;28:196-201.
21. Yashiro M, Carethers JM, Laghi L, Saito K, Slezak P, Jaramillo E, Rubio C, Koizumi K, Hirakawa K, Boland CR. Genetic pathways in the evolution of morphologically distinct colorectal neoplasms. Cancer Res 2001;61:2676-83.
22. Nakagoe T, Nanashima A, Sawai T, Tuji T, Ohbatake M, Jibiki M, Yamaguchi H, Kurosaki N, Yasutaka T, Ayabe H, Miyashita H, Arisawa K. Biological differences between polypoid and nonpolypoid growth types of colorectal cancer. Acta Med Nagasaki 2000;45:51-9.
23. Jen J, Powell SM, Papadopoulos N, Smith KJ, Hamilton SR, Vogelstein B, Kinzler KW. Molecular determinants of dysplasia in colorectal lesions. Cancer Res 1994;54:5523-6.
24. Nucci MR, Robinson CR, Longo P, Campbell P, Hamilton SR. Phenotypic and genotypic characteristics of aberrant crypt foci in human colorectal mucosa. Hum Pathol 1997;28:1396-407.
25. Gillies RJ, Kinahan PE, Hricak H. Radiomics: Images Are More than Pictures, They Are Data. Radiology 2016;278:563-77.
26. Horvat N, Veeraraqhavan H, Khan M, Blazic I, Zhenq J, Capanu M, Sala E, Garcia-Aquilar J, Gollub MJ, Petkovska I. MR Imaging of Rectal Cancer: Radiomics Analysis to Assess Treatment Response after Neoadjuvant Therapy. Radiology 2018;287:833-43.
27. Yeo DM, Oh SN, Jung CK, Lee MA, Oh ST, Rha SE, Jung SE, Byun JY, Gall P, Son Y. Correlation of dynamic contrast-enhanced MRI perfusion parameters with angiogenesis and biologic aggressiveness of rectal cancer: Preliminary results. J Magn Reson Imaging 2015;41;474-80.
28. Hong HS, Kim SH, Park HJ, Park MS, Kim KW, Kim WH, Kim NK, Lee JM, Cho HJ. Correlations of dynamic contrast-enhanced magnetic resonance imaging with morphologic, angiogenic, and molecular prognostic factors in rectal cancer. Yonsei Med J 2013;54:123-30.
29. Kim SH, Lee HS, Kang BJ, Song BJ, Kim HB, Lee H, Jin MS, Lee A. Dynamic contrast-enhanced MRI perfusion parameters as imaging biomarkers of angiogenesis. PLoS One 2016;11:e0168632.
30. Rak J, Mitsuhashi Y, Bayko L, Filmus J, Shirasawa S, Sasazuki T, Kerbel RS. Mutant ras oncogenes upregulate VEGF/VPF expression: implications for induction and inhibition of tumor angiogenesis. Cancer Res 1995;55:4575-80.
31. Cushman-Vokoun AM, Stover DG, Zhao Z, Koehler EA, Berlin JD, Vnencak-Jones CL. Clinical utility of KRAS and BRAF mutations in a cohort of patients with colorectal neoplasms submitted for microsatellite instability testing. Clin Colorectal Cancer 2013;12:168-78.

Cite this article as: Jo SJ, Kim SH. Association between oncogenic RAS mutation and radiologic-pathologic findings in patients with primary rectal cancer. Quant Imaging Med Surg 2019;9(2):238-246. doi: 10.21037/qims.2018.12.10

